Journal of Hydrology 632 (2024) 130874

Contents lists available at ScienceDirect

Journal of Hydrology

journal homepage: www.elsevier.com/locate/jhydrol

Research papers

Climate change leads to an expansion of global drought-sensitive area

Qiaoqiao Li [a,b], Aizhong Ye [a,*], Yoshihide Wada [b], Yuhang Zhang [a,c], Junju Zhou [d]

[a] State Key Laboratory of Earth Surface Processes and Resource Ecology, Faculty of Geographical Science, Beijing Normal University, Beijing 100875, China
[b] Biological and Environmental Science and Engineering Division, King Abdullah University of Science and Technology, Thuwal 23955, Saudi Arabia
[c] Department of Infrastructure Engineering, The University of Melbourne, Parkville 3010, Australia
[d] College of Geography and Environment Science, Northwest Normal University, Lanzhou 730070, China

ARTICLE INFO

This manuscript was handled by Yuefei Huang, Editor-in-Chief, with the assistance of Shanshui Yuan, Associate Editor

Keywords:
Drought propagation
Drought partitions
Agricultural drought
Drought-sensitive area expands
Climate change

ABSTRACT

Droughts will occur more extensively and frequently worldwide, where the increase in drought-sensitive area will further threaten the stability of global ecosystems. However, the distribution and changes of the drought-sensitive area remain unclear. Here we found the distribution and changes of the drought-sensitive area, humid type partition, and arid type partition of the propagation of meteorological drought to agricultural drought during the last 40 years via drought propagation analysis. We show that, globally, drought-sensitive area have increased significantly by 120×10^4 km^2, an area equivalent to The Republic of South Africa (122×10^4 km^2), while the humid type partition has decreased significantly by 384×10^4 km^2 which is larger than that of India (329×10^4 km^2). It indicates that the risk of drought is increasing significantly globally. Asia and South America are facing the most critical situation among the continents. Notably, the increase of drought-sensitive area and the loss of humid type partition were concentrated in their transition areas, and 6.44 % of humid type partition are changing into drought-sensitive area globally. In these transformation areas, the largest area is forested and agricultural land, which will seriously threaten the stability of the global ecosystem and food security.

1. Introduction

Drought severely affects energy production, food, water, and a range of socio-economic activities (Mishra and Singh, 2010; Mondal et al., 2023). Numerous studies have shown that, in the background of global warming, droughts are becoming more frequent, prolonged, and severe (Yin et al., 2023; Zhou et al., 2023).

Droughts usually start with insufficient rainfall (meteorological drought) and propagate through the hydrological cycle over a period of time to affect soil moisture (agricultural drought) and then runoff, groundwater aquifers, and water reservoirs (hydrological drought) (Zhang et al., 2022a; Van Loon et al., 2013). Human communities and food security are threatened by severe agricultural droughts (Mishra and Singh, 2010; Zhang et al., 2021a, 2021b; Yang et al., 2020). More notably, under CMIP6 future projections emission scenarios, agricultural droughts are at serious risk in different regions of the globe (Jiang and Zhou. 2023; Zhang et al., 2023; Yang et al., 2023; Bouabdelli et al., 2022; Lu et al., 2019).

The drought-sensitive area is a crucial region deserving considerable attention. Current drought sensitivity studies have focused on evaluating the sensitivity of ecosystems or species to drought in a certain region to determine the extent to which drought affects ecosystems and carbon cycling processes, such as vegetation (Jiang and Zhou. 2023; Sun et al., 2023), forests (Zhang et al., 2022b; Anderegg et al., 2020; Hoffmann et al., 2018; Scherrer et al., 2011), grasslands (Knapp et al., 2015), maize (Lobell et al., 2014), and so on. The study of ecosystem sensitivity to drought is necessary for ecosystem stabilization. Spatial information is important for the diagnosis of drought-related phenomena, and ecologists must study spatial patterns to enrich their understanding of the spatial processes occurring in the environment (Lin et al., 2011). Many scholars have made efforts to locate drought-sensitive area, for example, by constructing a system of indicators related to ecosystem functions to assess ecosystems and thus classify drought-sensitive areas (Li et al., 2022; Yan et al., 2016). Or, the Geographic Information System (GIS) and Remote Sensing (RS) techniques are used to classify drought-sensitive areas (Lin et al., 2011), and so on. At the same time, scientists have demonstrated that different regions have different sensitivities to the occurrence of droughts; For example, the risk of extreme events and

* Corresponding author at: State Key Laboratory of Earth Surface Processes and Resource Ecology, Faculty of Geographical Science, Beijing Normal University, Beijing 100875, China.
E-mail address: azye@bnu.edu.cn (A. Ye).

https://doi.org/10.1016/j.jhydrol.2024.130874
Received 27 September 2023; Received in revised form 3 January 2024; Accepted 24 January 2024
Available online 16 February 2024

aridification is greater in arid and semi-arid regions (Fu et al., 2008; Zhao et al., 2020). Especially in semi-arid regions, which are particularly sensitive to climate change (Huang et al., 2017; Poulter et al., 2014). However, the current positioning of drought-sensitive area is vague and inconsistent. At a time when drylands are in danger of expanding and droughts are occurring more rapidly faster, it is urgent to locate drought-sensitive areas on a global scale.

Ultimately, global vegetation and ecosystem services are highly dependent on soil moisture availability (Li et al., 2022). In the context of global change, the sensitivity of vegetation to soil moisture is generally increasing (Li et al., 2022; Gampe et al., 2021; Reichstein et al., 2013). Therefore, studying the sensitivity of soil moisture (agricultural drought) is important for both global ecosystem stability and food security. Using the concept of drought propagation to explore sensitive areas is an approach that can be tried. The propagation process of the same degree of meteorological drought events is different in various parts of the world and can lead to different agricultural drought events (Apurv et al., 2017). Identifying potential hotspots where agricultural drought is highly sensitive to meteorological drought (where agricultural drought is particularly sensitive to changes in meteorological drought) is crucial in aiding decision-makers to develop optimal strategies for drought prevention and response, and for controlling the expansion of drought areas in sensitive areas. At the global scale, exploring the spatial distribution and trends of drought-sensitive area remains a large gap.

Currently, there have been significant milestones in drought propagation research. Most researchers study the propagation process of meteorological drought to other drought types from the perspective of drought propagation time. This includes analyses of drought propagation time in various global regions (Mo et al., 2011; Huang et al., 2015; Zhang et al., 2021b; Xu et al., 2021), enhancements to the calculation method of drought propagation time (Li et al., 2022a; Zhou et al., 2021b) and explore the influencing factors affecting drought propagation time (Zhang et al., 2022c). However, there are obvious gaps. Firstly, the intensity and duration of agricultural droughts directly affect the stability of ecosystems compared to when meteorological droughts affect agricultural droughts. Therefore, it is crucial to shift the focus from solely the propagation time to also include the intensity and duration of agricultural drought events resulting from meteorological drought events. Secondly, most of the current studies have focused on regional or watershed scales and lack comparisons between different physical geographies on a global scale. An integrated exploration of drought propagation processes in terms of the drought characteristics of the drought itself should be given attention. Drought intensity and duration are indicators of drought severity. Based on the drought propagation index, the globe can be divided into partitions where the propagation of meteorological drought to agricultural drought is of equal intensity and duration (drought-sensitive area) and partitions where it is not (Zhou et al., 2019; Li et al., 2022b). A feasible method and attempt are provided to solve the above hypothesis. Applying this on a global scale and exploring the temporal and spatial variations of drought-sensitive areas can offer new insights into clarifying the drought propagation process.

Here, we calculate the global spatial distribution of drought partitions from 1981 to 2020 and simulate the year-to-year changes of drought partitions using the random forest algorithm. Then analyze the temporal and spatial trends and impact mechanisms of drought partitions, especially drought-sensitive area, to provide crucial insights for clarifying the causes of drought occurrence and development.

2. Material and methods

2.1. Data

2.1.1. Climate data

The meteorological datasets (precipitation, temperature, total evapotranspiration, and potential evapotranspiration) used in this research were derived from ERA5-Land Reanalysis data provided by the European Centre for Medium-Range Weather Forecasts (ECMWF). We used the period of 1981 to 2020 at a monthly temporal resolution and a spatial resolution of 0.1°. The data are publicly available and widely used (Zhou et al., 2021a, 2021b; Pelosi et al., 2020).

2.1.2. Soil moisture data

In this research, we focused on the analysis of topsoil drought. Data were obtained using volumetric soil water (0—–7 cm) data from ERA5-Land. We used the period of 1981 to 2020 at a monthly temporal resolution and a spatial resolution of 0.1°. The agricultural drought index is calculated using soil moisture data. The data are publicly available.

2.1.3. DEM data

The DEM data use the Multiple Error Removal Improved Terrain Mapping (MERIT DEM) dataset, which has a spatial range between 90 N and 60 S and a spatial resolution of 3 sec. We have resampled the spatial resolution to 0.1 degrees to achieve a spatial match. The data are publicly available.

2.1.4. Land cover data

The NDVI data we used the Global GIMMS NDVI3g v1, which was published by the NOAA Global Inventory Monitoring and Modeling System (GIMMS) in a period from 1981 to 2015 (Pinzon et al., 2014; Tucker et al., 2005). This data are publicly available.

ESA CCI Global Land Cover product was used in this study. The time scale is 1992–2015 and the spatial resolution is 300 m. The land cover classification of this dataset using the UN-LCCS was defined to meet a variety of models and practical applications. To achieve a spatial match we unified the resolution of all influencing factors to 0.1 degree. This data is publicly available (Defourny et al., 2017).

2.2. Methods

2.2.1. Drought index

We used the Standardized Precipitation Index (SPI) (Mckee et al., 1993) for meteorological drought and the Standardized Soil Moisture Index (SSMI) (Sheffield et al., 2004) for agricultural drought. The SSMI can be defined similar to the commonly used SPI that has been used in a wide variety of studies, which uses the normal quantile transformation to standardize the index (specifically to make the drought index spatiotemporally comparable) (Zhu et al., 2021). The difference between the two is that SPI takes precipitation as its parameter input while SSMI takes soil moisture as its parameter input. SSMI and SPI have multiple timescales, with each representing various drought and flood conditions.

The drought propagation index is a variable that quantifies the process of propagation of drought features (Li et al., 2022b). The improved Drought Duration Propagation Index (DDP) and Drought Intensity Propagation Index (DIP) were selected to represent the propagation of drought duration and drought intensity, respectively, during the propagation of meteorological drought to agricultural drought.

The formulae are:

$$\mathrm{DDP} = \frac{\mathrm{SD}_{\mathrm{SSMI1-Ln}}}{\mathrm{MD}_{\mathrm{SPIn-Ln}}} (\mathrm{MD} \neq 0) \tag{1}$$

$$\mathrm{DIP} = \frac{\mathrm{SI}_{\mathrm{SSMI1-Ln}}}{\mathrm{MI}_{\mathrm{SPIn-Ln}}} (\mathrm{MI} \neq 0) \tag{2}$$

where n represents the dry-wet meteorological to dry-wet agricultural propagation time. In this study, the Pearson correlation coefficient (PCC) was chosen to ascertain the propagation time (PT) from meteorological drought to agricultural drought. The SPI accumulation period (n) corresponding to the maximum Pearson correlation coefficient was used as the PT of meteorological drought to agricultural drought.

$MI_{SPIn-Ln}$ and $SI_{SSMI1-Ln}$ are the mean values of the drought sequences corresponding to SPI and SSMI, respectively, and $MD_{SPIn-Ln}$ and $SD_{SSMI1-Ln}$ are the total drought duration of the drought sequences corresponding to SPI and SSMI, respectively. For detailed calculations, please refer to the reference (Li et al., 2022b). The grading of the drought propagation index is shown in Table 1:

2.2.2. Drought partition

By combining the DIP and DDP classifications, the global drought partition (DP) can be classified into nine regions. The specific division is shown in Table 2. We focus on exploring the three key drought partitions, Drought-sensitive area (per-per type drought propagation partition, P-P V), Arid type partition (arid type drought propagation partition, Arid I), and Humid type partition (humid type drought propagation partition, Humid IX). The partitioning standards are specified as shown in Table 2:

In the humid type partition, where the meteorological drought intensity is weaker than agricultural drought intensity (DIP > 1.1) and meteorological drought duration is higher than agricultural drought duration (DDP < 0.9), In this region, the duration of agricultural drought is shorter than that of meteorological drought, but the intensity and destructiveness of agricultural drought is high. In the arid type partition, where the meteorological drought intensity is greater than the agricultural drought intensity (DIP < 0.9) and the meteorological drought duration is short compared to the agricultural drought duration (DDP > 1.1), In this region, the intensity of the agricultural drought is low but the frequency of occurrence is high. In the drought-sensitive area, where the propagation of meteorological drought to agricultural drought is equivalent, and the duration and intensity of meteorological drought are close to those of agricultural drought. In this region, agricultural drought is sensitive to the response to meteorological drought. Except for these three drought partitions, other drought partitions are smaller in area and are not of concern for the time being.

We calculated the turning year of area change for each drought partition in each continent from 1981 to 2020. If the frequency of occurrence of a drought partition before the turning year in the grid point of that continent is less than 50 %, and the frequency of occurrence of that partition after the turning year is greater than 50 %, the grid point is defined as the increased area of this partition. Conversely, it defines the grid point as the lost area of this partition. A grid point is defined as a holding area for this partition if it occurs more than 50 % of the time in both the period before and after the turning year. When the trend of area change of a drought partition in a continent is not significant (P > 0.05), the turning year of global drought partition is used.

2.2.3. Mann-Kendall (M−K) trend test and turning year diagnosis

The Mann-Kendall (M−K) trend test is a non-parametric method recommended by the World Meteorological Organization for analyzing trends in time series. In this paper, $P < 0.05$ indicates that the series has a significant increasing or decreasing trend at the 0.05 confidence level, and $P < 0.01$ indicates that the series has a significant increasing or decreasing trend at the 0.01 confidence level (Güçlü et al., 2020; Kisi et al., 2014; Gocic et al., 2013).

The Cumulative Offset Verification (COV) method was utilized to diagnose the turning year. The COV method is a nonlinear statistical method to visually determine the trend of discrete data points from a curve. From the fluctuation of the curve, we can determine the turning year (Zhang et al., 2015; Weber et al., 2004).

Table 1
The grading of the drought propagation index.

DDP or DIP	Index range
(0,0.9)	Weak (w)
[0.9,1.1)	Peer-to-peer (p-p)
(1.1, +∞)	Strong (s)

Table 2
Division of drought partition.

DDP DIP	Strong	Peer-to-peer	Weak
Weak	Arid I	IV	VII
Peer-to-peer	II	P-P V	VIII
Strong	III	VI	Humid IX

2.2.4. Random forests

Random Forests (RF) is the most representative algorithm in the Bagimng integration method, which as published by Breiman in, 2001, is an algorithm based on classification trees. It raises prediction accuracy by combining numerous classification trees to create a “forest” without significantly increasing computational power (Li et al., 2013). The method exhibits a high tolerance for unusual values and noise, is not easily overfitted, and has a broad range of applications across multiple fields (Lu et al., 2012; Zhang et al., 2022d).

The simulation inference process of the RF model is as follows: firstly, given a training set F (Y_i, X_i) with N samples, Y_i represents the simulation's target variable and X_i is the feature variable with p dimensions, a training model is derived, followed by adjustment of the model parameters, and finally the simulation set is brought into the optimized model and simulated.

$$F(Y_i, X_i), i = 1, ..., N \tag{3}$$

$$X_i = X_i^1, X_i^2, X_i^3, ..., X_i^p \tag{4}$$

In this paper, the target variable Y_i in the training set is the value of the global drought partitions from 1981 to 2020 calculated using the drought propagation index. Because a lower number of classifications leads to more accurate simulated results, the drought partitions are consolidated into one type except for arid type partition, drought-sensitive area, and humid type partition. The chosen characteristic variables include precipitation, soil moisture, temperature, total evapotranspiration, potential evaporation, land use, NDVI, and DEM. For land use and land cover, the selected type corresponds to the one with the highest frequency at each grid point. The simulation dataset comprises yearly data for precipitation, soil moisture, temperature, total evaporation, and potential evaporation across 1.3 million global grid points from 1981 to 2020, and NDVI, land use and land cover, and DEM are consistent with the training set. Simulations using the optimized model yielded year-by-year drought partitions globally.

3. Results

3.1. Global drought partition from meteorological drought to agricultural drought propagation

We have used the Drought Duration Propagation Index (DDP) (Fig. 1a) and the Drought Intensity Propagation Index (DIP) (Fig. 1b) to classify the global drought partition (Fig. 1c). We focus on three key drought partitions: Humid type partition, Drought-sensitive area, and Arid type partition. Among these, the drought-sensitive area is the most widely distributed, covering 38 % of the globe (Fig. 1c, region V), in which the land–atmosphere interaction is strong (Dirmeyer, 2011; Gao, 2018; Hua et al., 2013; Wei et al., 2008) and further plays a role in regulating thermal conditions and influencing precipitation (Bellucci et al., 2015; Seneviratne et al., 2010), and where meteorological droughts have a direct impact on agricultural droughts, while agricultural droughts also greatly influence meteorological droughts.

Within the remaining drought partitions, agricultural drought is insensitive to variations in meteorological drought, and variations in the duration and intensity of meteorological drought have no significant impact on agricultural drought. Among these, the humid type partition covers 29 % of the global area (Fig. 1c, region I). In this region, water is

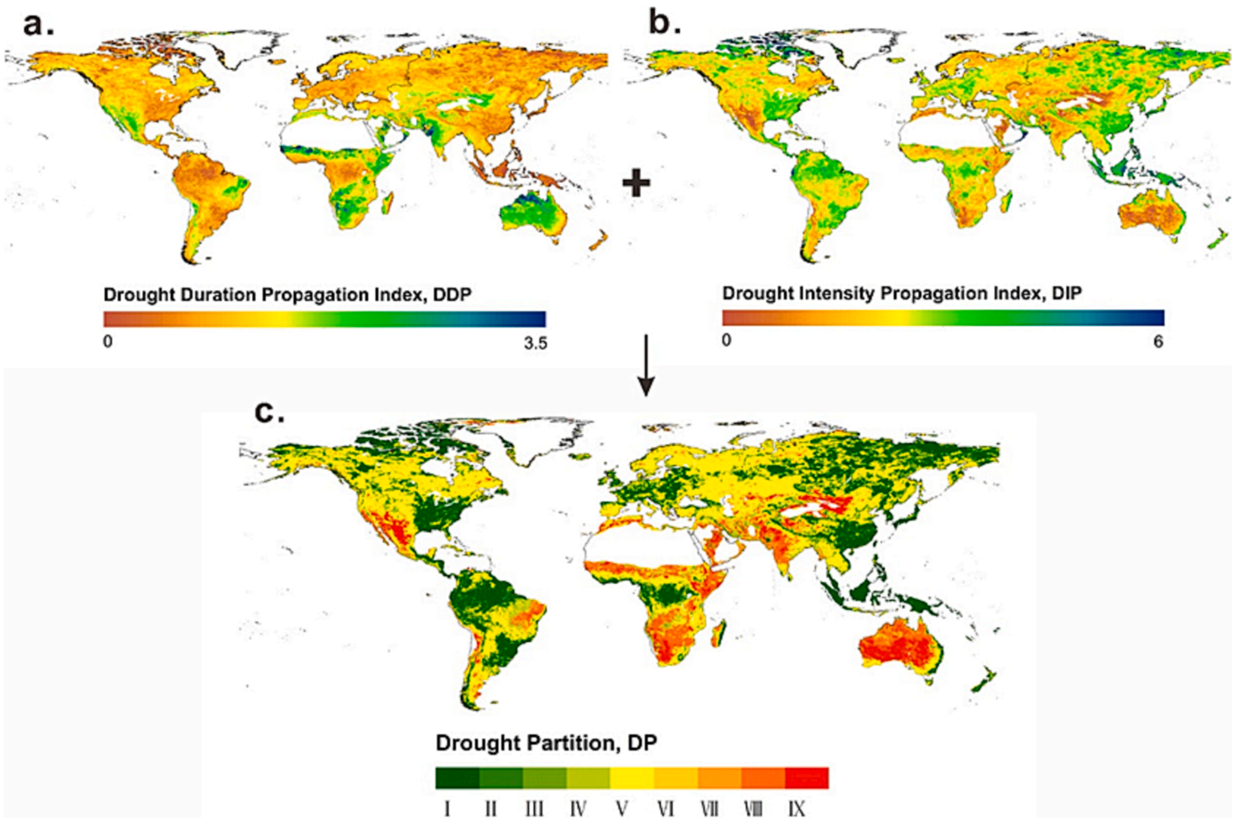

Fig. 1. **a.** Propagation of meteorological drought duration to agricultural drought for the years 1981 to 2020; **b.** Propagation of meteorological drought intensity to agricultural drought for the years 1981 to 2020; **c.** Spatial distribution of global drought partitions from 1981 to 2020 (I: Humid type drought propagation partition (Humid type partition); V: Per-per type drought propagation partition (Drought-sensitive area); IX: Arid type drought propagation partition (Arid type partition)).

sufficient and evaporation is determined by energy. The soil retains significant moisture and has a buffering effect against the onset of meteorological drought, which does not lead to a rapid decrease in soil moisture (Dirmeyer et al., 2006; Gao, 2018; Muñoz-Sabater et al., 2021). The roots of plants are well-developed, and they are more resilient to the change of dry-wet surface soil (Huang et al., 2015; Zhou et al., 2021a). The occurrence of meteorological drought does not necessarily trigger agricultural drought, but when meteorological drought leads to agricultural drought, the intensity of the agricultural drought is severe and the impact is significant.

The arid type partition covers 8 % of the global area (Fig. 1c, region IX). In this region, the geographical location of the region determines that water conditions are very tight, evaporation is determined by water (Gao, 2018; Liu et al., 2010; Zhang et al., 2001), soils may even be sandy (Gao, 2018), small amounts of precipitation are not sufficient to alleviate or affect agricultural drought (Wang, 2014), agricultural drought is insensitive to changes in meteorological drought. Apart from these three drought partitions, other drought partitions are smaller in area and are currently not a concern.

Spatially, the drought partitions in the middle and low-latitude regions are more consistent with the climatic regions. The drought-sensitive area is mainly located in semiarid and dry subhumid climate areas, with major land use types being woodland (38 %), grassland (29 %), and agricultural areas (24 %). The humid type partition is mainly located in the humid climate region, with major land use types being woodland (54 %) and agricultural area (23 %). The arid type partition is mainly located in the arid climate region, with major land use types being grassland (61 %) and bare land (23.5 %). In the higher latitudes, drought-sensitive area and humid type partition are dominant.

3.2. *Global drought-sensitive area are expanding*

We simulated the annual spatial distribution of drought partitions worldwide from 1981 to 2020 by using the random forest classification algorithm. We found that the area of the drought-sensitive area increased significantly ($P < 0.05$), the turning year was 2002. The average area of the drought-sensitive area from 2003 to 2020 increased by about 120×10^4 km^2 compared to 1981–2002 (Fig. 2), which is equivalent to the size of The Republic of South Africa (122×10^4 km^2), and the increase accounted for 3 % of the actual area of the drought-sensitive area. The area of the humid type partition had a significant tendency to decrease ($P < 0.05$), with the turning year was 2001. The average area before and after the turning year decreased by about 384×10^4 km^2 (Fig. 2), which is larger than that of India (329×10^4 km^2), and the reduced area accounted for 11.5 % of the humid type partition. The trend in the arid type partition was not significant (Fig. 2). The area sensitive to agricultural drought triggered by meteorological drought is expected to gradually increase, which will seriously threaten the stability of global ecosystems and food security.

The trends in the area and the year of mutation vary for each drought partition on every continent (Table 3). Specifically, only in Asia and South America, the area of the humid type partition disappear significantly, and the area of the drought-sensitive area increases significantly, indicating these continents are facing the most severe situation, and the entire continent's ecosystem is becoming progressively more sensitive. Among these, the humid type partition in South America experienced the largest loss of area, totaling 154×10^4 km^2, accounting for 20.7 % of the actual humid type partition area of the continent, Simultaneously, the drought-sensitive area saw the largest percentage increase of 10.7 %. Although the area of the humid type partition Asia decreases more and the proportion of this area is the smallest (7 %), the drought-sensitive area increases the most, reaching 67×10^4 km^2. The area of both the

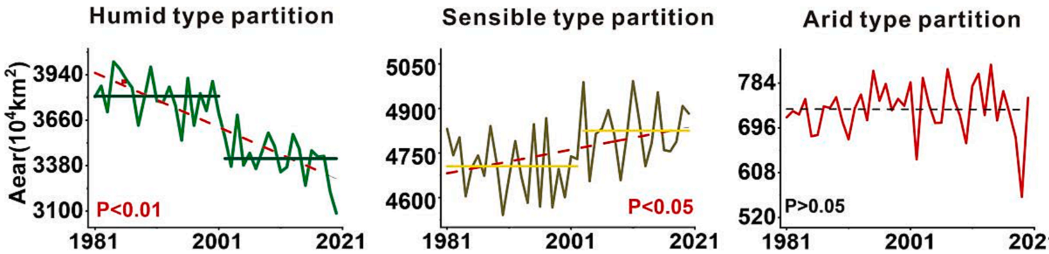

Fig. 2. Trends in the area of key drought partitions at global and continental scales from 1981 to 2020 (Red color indicates a significant change trend). (For interpretation of the references to color in this figure legend, the reader is referred to the web version of this article.)

Table 3
Characteristics of changes in each drought partition for each continent.

Continent	Key drought partitions	Trend	P-value	Turning year	Area changes ($\times 10^4$ km^2)	Proportion of the area of the drought partition (%)
Asia	Humid	Downward	$P < 0.05$	2006	−100	−7.19
	Sensible areas	Upward	$P < 0.05$	2006	+74	4.84
South America	Humid	Downward	$P < 0.01$	2002	−154	−20.75
	Sensible areas	Upward	$P < 0.01$	2002	57	10.69
Europe	Humid	Downward	$P > 0.05$	2001	−30	−11.44
	Sensible areas	Upward	$P > 0.05$	2002	26	4.42
North America	Humid	Downward	$P < 0.01$	1997	−67	−10.64
	Sensible areas	Downward	$P > 0.05$	2002	3	0.3
Africa	Humid	Downward	$P < 0.01$	2000	−63	−22.6
	Sensible areas	Downward	$P > 0.05$	2002	−2	−0.34
Oceania	Humid	Downward	$P < 0.05$	1992	−8	−15.31
	Sensible areas	Downward	$P < 0.01$	2001	−22	−19.68

humid type partition and the drought-sensitive area in Oceania decreased significantly, with the maximum percentage reduction percentage observed in the drought-sensitive area at 19.7 %.

Africa and North America showed a significant decreasing trend in the area of the humid type partition, but the trend in the area of the drought-sensitive area was not significant. The largest percentage of areas with reduced humid type partition in Africa was 22.6 %. None of the area trends of the European drought partitions were significant. In summary, South America's situation has become even more serious, with the entire continent's ecosystems becoming progressively more sensitive.

3.3. Global drought-sensitive area increase from humid type partition

For better and more accurate early warning of droughts, we further analyzed the spatial locations of the area increased, lost, and holding areas of humid type partition and drought-sensitive areas in each continent (Fig. 3a). The increased areas of drought-sensitive area are primarily concentrated in the areas of its transition with the humid type partition, and the decreased areas of drought-sensitive area are primarily concentrated in the areas of its transition with the arid type partition. There is an interconversion of the area of the three key drought partitions, and the ecosystems in these transformed areas are facing more serious challenges. Among them, 56 % of the loss area of the humid type partition was transformed into a drought-sensitive area, and 22.9 % of the increased area of the arid type partition was transformed from a drought-sensitive area. From this, we can see that the world is facing a situation where the humid areas become sensitive and the sensible areas become arid.

The transformed areas from humid type partition to drought-sensitive area is the largest, while according to the current development trend, the area will further expand. We should focus on transformed areas to prepare for possible future changes. Typical areas of these transformed areas are distributed on all continents (Fig. 3). For example, in the Central Siberian Plateau in Asia, the main land use types are coniferous forests (44 %) and steppes (11.6 %). The region of agricultural land (63 %) in the Volyn-Podilsk Upland in the territory of Ukraine and the Paris Basin in the western part of the Western European Plain in Europe. Broadleaf forests (66 %) in the southern, western, and northern ring-margin areas of the Congo Basin in Africa. Broadleaf forests (50.1 %) and scrub areas (14.3 %) in the Great Divide of Oceania. The southern edge of the Amazon Plain-Paraguay Basin-La Plata Plain-Pampas region of South America, where the main land use types are evergreen deciduous forest (34 %), agricultural land (15.6 %) and scrub (11.3 %). In North America, lichens and mosses (25.5 %) in the area north of 60°N, grasslands (10 %), and agricultural lands (7.6 %) in the range 30-40°N 99-93°W in the Great Plains. The largest proportion of transformation areas worldwide is forest (47 %), followed by agricultural land (18.5 %), which will seriously threaten global ecosystem stability and food security.

4. Discussion

The main impact mechanisms are different for each drought partition (Fig. 4). As previously stated, evapotranspiration is limited by moisture conditions in the arid type partition and by energy in the humid type partition. Only in drought-sensitive areas does soil moisture play a role in regulating thermal conditions and influencing precipitation due to land–atmosphere interactions (Bellucci et al., 2015; Seneviratne et al., 2010). Drought-sensitive regions are primarily focused in areas of transition of dry-wet climatic conditions and are areas where land–atmosphere interaction is particularly strong (Wei et al., 2008; Hua et al., 2013; Gao, 2018; Dirmeyer, 2011). Soil moisture has a controlling effect on evapotranspiration, which influences surface energy distribution (Bellucci et al., 2015; Seneviratne et al., 2010). In drought-sensitive areas, the value of precipitation lies between potential and actual evapotranspiration, where a portion of the precipitation affects soil moisture. In this region, meteorological drought has a direct and significant impact on agricultural drought through land–atmosphere interactions. In addition, ecosystems in drought-sensitive areas have a degree of vulnerability. Among the continents, Europe has the largest proportion of drought-sensitive area (62 %), showing that agricultural drought is highly sensitive to the occurrence of meteorological droughts across the continent. This explains the particularly strong soil water

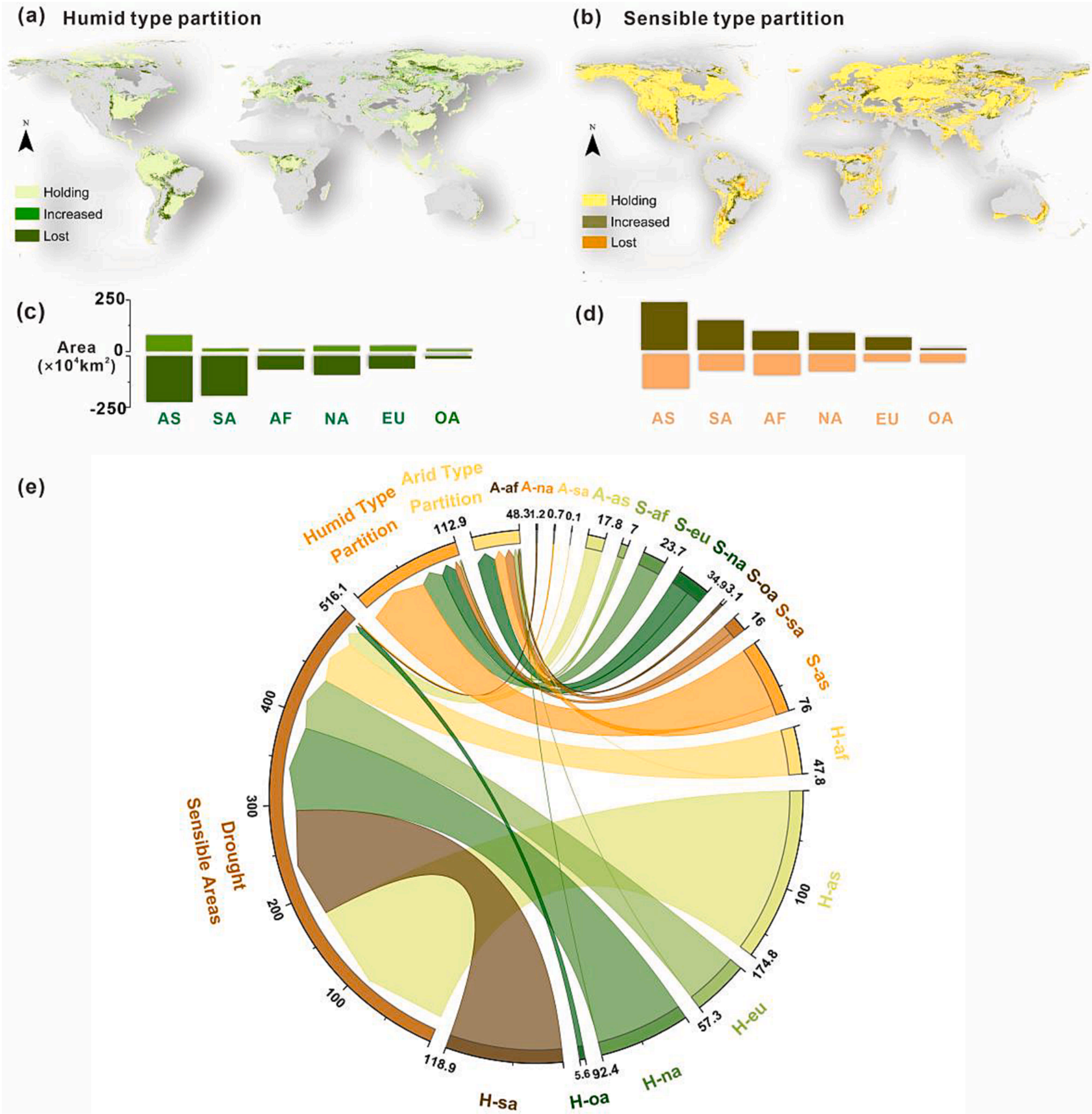

Fig. 3. Spatial variation characteristics of global humid type partition and drought-sensitive area before and after turning year (**a.** Spatial divisions of area increased, lost, and holding before and after turning year in the humid type partition; **b.** Spatial divisions of the area increased, lost, and holding before and after turning year in the drought-sensitive area; **c.** The area of increase and decrease of the humid type partition before and after the turning year in each continent (AF: Africa, NA: North America, AS: Asia, SA: South America, EU: Europe, OA: Oceania); **d.** The area of increase and decrease of drought-sensitive area before and after the turning year in each continent.); e. Area of transition of the lost area in different drought partitions to other drought partitions (unit:10^4 km^2, H: Humid type partition, S: Drought-sensitive area, A: Arid type partition).

deficit and more severe drought in Europe compared to other regions in a global warming context (Rousi et al., 2022; Vogel et al., 2017; Miralles et al., 2014; Seneviratne et al., 2010).

The major driver of the rapid loss of the global humid type partition and the significant increase in the area of the drought-sensitive area is climate change (Fig. 4b). Climate changing signals include higher temperatures, increased evaporation losses, reduced snowfall and snow cover, as well as heightened soil moisture deficits and runoff (Cook et al., 2018). At the same time, global climate change further exacerbates land–atmosphere feedbacks, directly or indirectly increasing the frequency of drought events. (Dirmeye, 2013; Alizadeh, 2020).

Other factors influence the process of drought propagation by affecting the local climate. The highest trend of transformation from humid type partition to drought-sensitive area in South America may be due to the massive deforestation of tropical forests (Kaplan et al., 2011; Pongratz et al., 2008; Ramankutty et al., 1999). Since the 2000 s, the consequences of heavy rainforest deforestation have gradually emerged, most notably in the form of changes in surface biophysical properties (Li et al., 2015; Davin et al., 2010; Bonan et al., 2008), leading to regional warming and drying (Smith et al., 2023; Lawrence et al., 2015; Costa

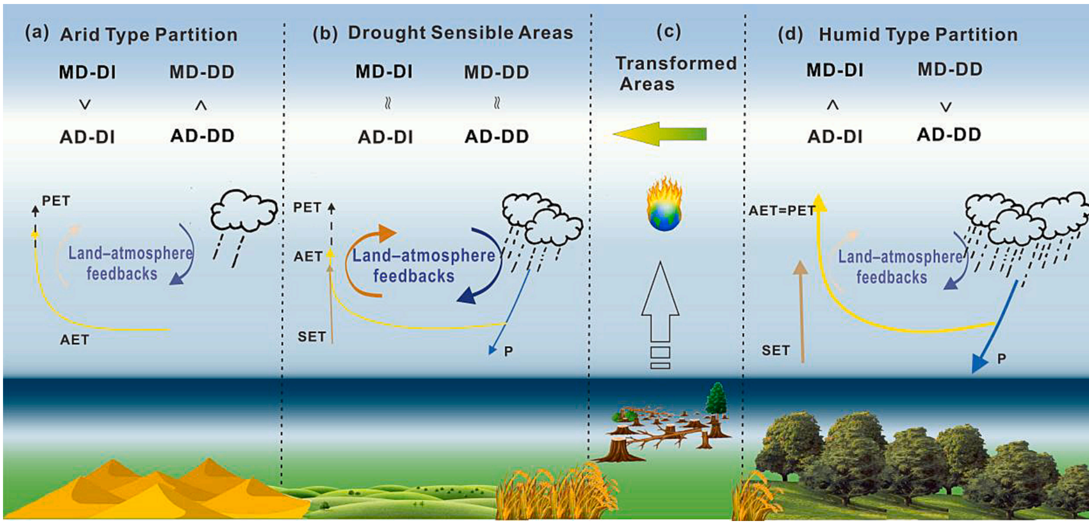

Fig. 4. Factors influencing of drought partition. (**a.** Arid type partition (MD: Meteorological Drought, AD: Agricultural Drought, DI: Drought Intensity, DD: Drought Duration, PET: potential evaporation, AET: Actual evaporation, SET: Soil evaporation, P: Precipitation); **b.** Drought-sensitive area; **c.** Transformed areas: the area transformed from a humid type partition to a drought-sensitive area; **d.** Humid type partition).

et al., 2000; Zhang et al., 1996). Deforestation of tropical rainforests responds differently on each continent. Many studies using climate models generally conclude that Amazonian logging has the greatest impact on climate change of any continent (Li et al., 2022c; Kooperman et al., 2018; Mahmood et al., 2014). This explains the significant decrease in the area of humid type partition, the significant increase in the area of drought-sensitive area in South America, and the rapid rate of change. It also explains the non-significant increase in the area of drought-sensitive area in the Congo Basin in Africa, despite the significant loss in Humid type partition.

Finally, this study provides a preliminary breakdown of the spatial and temporal variability and attribution of the global drought-sensitive area, which offers new ideas for studying the drought propagation process. However, the main consideration was the impact of climate variability on the distribution of drought, and other influencing factors can be added in the future research process, such as taking into account the impact of human activities on the partitioning of droughts.

5. Conclusions

The increase in the drought-sensitive area will seriously threaten the stability of global ecosystems. This study uses the drought propagation method to explore the distribution and variation of drought propagation from global meteorological drought to agricultural drought propagation.

The results show that the drought-sensitive area is the most widely distributed globally and agricultural drought in this area is more sensitive to meteorological drought. Drought partitions in the middle and low-latitude regions show a high degree of consistency with climatic regions, and the drought-sensitive area is mainly focused in semi-arid and dry sub-humid climates. Over the past 40 years, globally, there has been an increase of 120×10^4 km^2 in the area of drought-sensitive area (equivalent to the area of The Republic of South Africa) and the area of the humid type partition (humid type drought propagation partition) has decreased by 384×10^4 km^2 (an area larger than India). Among the continents, Asia and South America are facing the most critical situation, the area of humid type partition shows a significant decreasing trend, and the area of drought-sensitive area shows a significant increasing trend. It is noteworthy that 58 % of the area of the drought-sensitive area increase is transformed from the humid type partition.

With global climate change, the world faces the risk of gradually becoming progressively more sensitive and arid, and previously stable soil moisture may become sensitive to meteorological drought. Soils in areas that were previously sensitive to meteorological drought may become progressively degraded, with irreversible consequences. Meanwhile, in the transformation area, the food-producing area accounts for a relatively large area, which will seriously threaten global food security. The development of the drought-sensitive area should be the focus of future research.

CRediT authorship contribution statement

Qiaoqiao Li: Writing – review & editing, Writing – original draft, Software, Methodology, Formal analysis, Data curation. **Aizhong Ye:** Writing – review & editing, Resources, Project administration, Funding acquisition, Conceptualization. **Yoshihide Wada:** Writing – review & editing, Validation, Formal analysis. **Yuhang Zhang:** Writing – review & editing, Validation, Data curation. **Junju Zhou:** Writing – review & editing, Validation, Data curation.

Declaration of competing interest

The authors declare that they have no known competing financial interests or personal relationships that could have appeared to influence the work reported in this paper.

Data availability

Data will be made available on request.

Acknowledgments

This study was supported by the Natural Science Foundation of China (No. 42171022), the Second Tibetan Plateau Scientific Expedition and Research Program (No.2019QZKK0405), and the China Scholarship Council (No.202306040129).

Author contributions

Q. Li and A. Ye designed the research; Q. Li collected the data; Q. Li, Y. Wada, J. Zhou, and A. Ye performed the analyses; and Q. Li, A. Ye, Y. Wada, J. Zhou, and Y. Zhang. wrote the manuscript.

References

Alizadeh, M.R., Adamowski, J., Nikoo, M.R., AghaKouchak, A., Dennison, P., Sadegh, M., 2020. A century of observations reveals increasing likelihood of continental-scale compound dry-hot extremes. Sci. Adv. 6 (39), eaaz4571. https://doi.org/10.1126/sciadv.aaz4571.

Anderegg, W.R., Trugman, A.T., Badgley, G., Konings, A.G., Shaw, J., 2020. Divergent forest sensitivity to repeated extreme droughts. Nat. Clim. Chang. 10 (12), 1091–1095.

Apurv, T., Sivapalan, M., Cai, X., 2017. Understanding the role of climate characteristics in drought propagation. Water Resour. Res. 53 (11), 9304–9329. https://doi.org/10.1002/2017WR021445.

Bellucci, A., Haarsma, R., Bellouin, N., Booth, B., Cagnazzo, C., van den Hurk, B., et al., 2015. Advancements in decadal climate predictability: The role of nonoceanic drivers. Rev. Geophys. 53 (2), 165–202. https://doi.org/10.1002/2014RG000473.

Bonan, G.B., 2008. Forests and climate change: forcings, feedbacks, and the climate benefits of forests. Science 320 (5882), 1444–1449. https://doi.org/10.1126/science.1155121.

Bouabdelli, S., Zeroual, A., Meddi, M., Assani, A., 2022. Impact of temperature on agricultural drought occurrence under the effects of climate change. Theor. Appl. Climatol. 148 (1–2), 191–209. https://doi.org/10.1007/s00704-022-03935-7.

Breiman, L., 2001. Random forests. Mach. Learn. 45 (1), 5–32. https://doi.org/10.1023/a:1010933404324.

Cook, B.I., Mankin, J.S., Anchukaitis, K.J., 2018. Climate change and drought: from past to future. Current Climate Change Reports 4, 164–179. https://doi.org/10.1007/s40641-018- 0093-2.

Costa, M.H., Foley, J.A., 2000. Combined effects of deforestation and doubled atmospheric CO2 concentrations on the climate of Amazonia. J. Clim. 13 (1), 18–34. https://doi.org/10.1175/15200442(2000)013<0018:CEODAD>2.0.CO;2.

Davin, E.L., de Noblet-Ducoudré, N., 2010. Climatic impact of global-scale deforestation: radiative versus nonradiative processes. J. Clim. 23 (1), 97–112. https://doi.org/10.1175/2009JCLI3102.1.

Defourny, P., Lamarche, C., Bontemps, S., De Maet, T., Van Bogaert, E., Moreau, I., Brockmann, C., Boettcher, M., Kirches, G., Wevers, J., Santoro, M., Ramoino, F., and Arino, O. (2017). Land Cover Climate Change Initiative - Product User Guide v2. Issue2.0.http://maps.elie.ucl.ac.be/CCI/viewer/download/ESACCI-LC-Ph2- P UGv2_2.0.pdf.

Dirmeyer, P.A., Koster, R.D., Guo, Z., 2006. Do global models properly represent the feedback between land and atmosphere. J. Hydrometeorol. 7 (6), 1177–1198. https://doi.org/10.1175/JHM532.1.

Dirmeyer, P.A., Jin, Y., Singh, B., Yan, X., 2013. Evolving land–atmosphere interactions over North America from CMIP5 simulations. J. Clim. 26 (19), 7313–7327. https://doi.org/10.1175/JCLI-D-12-00454.1.

Dirmeyer, P. A. (2011). The terrestrial segment of soil moisture-climate coupling. Geophysical Research Letters, 38(16), LI6702. https://doi.org/10.1029/2011G L048268.

Fu, C., Jiang, Z., Guan, Z., He, J., Xu, Z.F., 2008. Regional climate studies of China. (Springer Science and Business Media.

Gampe, D., et al., 2021. Increasing impact of warm droughts on northern ecosystem productivity over recent decades. Nat. Clim. Chang. 11, 772–779.

Gao, C.J., 2018. Regional differences in land-atmosphere coupling and possible impacts of soil moisture over. Nanjing University of Information Science and Technology (In Chinese), Eastern China.

Gocic, M., Trajkovic, S., 2013. Analysis of changes in meteorological variables using mann-kendall and sen's slope estimator statistical tests in Serbia. Global Planet. Change 100, 172–182. https://doi.org/10.1016/j.gloplacha.2012. 10.014.

Güçlü, Y.S., 2020. Improved visualization for trend analysis by comparing with classical mann-kendall test and ITA. J. Hydrol. 584, 124674 https://doi.org/10.1016/j.jhydrol.2020.124674.

Hoffmann, N., Schall, P., Ammer, C., Leder, B., Vor, T., 2018. Drought sensitivity and stem growth variation of nine alien and native tree species on a productive forest site in Germany. Agric. For. Meteorol. 256, 431–444.

Hua, W., Chen, H., Zhu, S., Sun, S., Yu, M., Zhou, L., 2013. Hotspot of the sensitivity of land surface hydrological cycle to climate change. Chin. Sci. Bull. 58 (30), 3682–3688. https://doi.org/10.1007/s11434-013-5846-7.

Huang, S.Z., Huang, Q., Chang, J.X., Leng, G., Xing, L., 2015. The response of agricultural drought to meteorological drought and the influencing factors: a case study in the Wei River basin, China. Agric Water Manag 159, 45–54. https://doi.org/10.1016/j.agwat.2015.05.023.

Huang, J., Xie, Y., Guan, X., Li, D., Ji, F., 2017. The dynamics of the warming hiatus over the northern hemisphere. Clim. Dyn. 48, 429–446.

Jiang, J., Zhou, T., 2023. Agricultural drought over water-scarce Central Asia aggravated by internal climate variability. Nat. Geosci. 1–8 https://doi.org/10.1038/s41561-022- 01111-0.

Kaplan, J.O., Krumhardt, K.M., Ellis, E.C., Ruddiman, W.F., Lemmen, C., Goldewijk, K.K., 2011. Holocene carbon emissions as a result of anthropogenic land cover change. The Holocene 21 (5), 775–791. https://doi.org/10.1177/0959683610386983.

Kisi, O., Ay, M., 2014. Comparison of mann-kendall and innovative trend method for water quality parameters of the Kizilirmak River, Turkey. J. Hydrol. 513, 362–375. https://doi.org/10.1016/j.jhydrol.2014.03.005.

Knapp, A.K., Carroll, C.J., Denton, E.M., La Pierre, K.J., Collins, S.L., Smith, M.D., 2015. Differential sensitivity to regional-scale drought in six central US grasslands. Oecologia 177, 949–957.

Kooperman, G.J., Chen, Y., Hoffman, F.M., Koven, C.D., Lindsay, K., Pritchard, M.S., Randerson, J.T., 2018. Forest response to rising CO2 drives zonally asymmetric rainfall change over tropical land. Nat. Clim. Chang. 8 (5), 434–440. https://doi.org/10.1038/s41558-018-0144-7.

Lawrence, D., Vandecar, K., 2015. Effects of tropical deforestation on climate and agriculture. Nat. Clim. Chang. 5 (1), 27–36. https://doi.org/10.1038/NCLIMATE2430.

Li, X., 2013. Using" random forest" for classification and regression. Chin. J. Appl. Entomol. 50 (4), 1190–1197.

Li, Y., Zhao, M., Motesharrei, S., Mu, Q., Kalnay, E., Li, S., 2015. Local cooling and warming effects of forests based on satellite observations. Nat. Commun. 6 (1), 6603. https://doi.org/10.1038/ncomms7603.

Li, Y., Brando, P.M., Morton, D.C., Lawrence, D.M., Yang, H., Randerson, J.T., 2022c. Deforestation-induced climate change reduces carbon storage in remaining tropical forests. Nat. Commun. 13 (1), 1964. https://doi.org/10.1038/s41467-022-29601-0.

Li, Y., Huang, S., Wang, H., Zheng, X., Huang, Q., Deng, M., Peng, J., 2022d. High-resolution propagation time from meteorological to agricultural drought at multiple levels and spatiotemporal scales. Agric Water Manag 262, 107428. https://doi.org/10.1016/j.agwat.2021.107428.

Li, W., Migliavacca, M., Forkel, M., Denissen, J.M., Reichstein, M., Yang, H., Orth, R., 2022b. Widespread increasing vegetation sensitivity to soil moisture. Nat. Commun. 13 (1), 3959.

Li, Q., Ye, A., Zhang, Y., Zhou, J., 2022a. The peer-to-peer type propagation from meteorological drought to soil moisture drought occurs in areas with strong land-atmosphere interaction. Water Resour. Res. 58 (9), e2022WR032846 https://doi.org/10.1029/2022WR032846.

Lin, M.L., Chen, C.W., 2011. Using GIS-based spatial geocomputation from remotely sensed data for drought risk-sensitive assessment. International Journal of Innovative Computing, Information and Control 7 (2), 657–668.

Liu, B., Xiao, Z.N., Ma, Z.G., 2010. Relationship between pan evaporation and actual evaporation in different humid and arid regions of China. Plateau Meteorology 29, 629–636. In Chinese.

Lobell, D.B., Roberts, M.J., Schlenker, W., Braun, N., Little, B.B., Rejesus, R.M., Hammer, G.L., 2014. Greater sensitivity to drought accompanies maize yield increase in the US Midwest. Science 344 (6183), 516–519.

Lu H and Feng Y. (2012). A review of random forests algorithm.Journal of the Hebei Academy of Sciences, 36(03):37-41. https://doi.org/10.16191/j.cnki.hbkx. 2019.03.005.

Lu, J., Carbone, G.J., Grego, J.M., 2019. Uncertainty and hotspots in 21st century projections of agricultural drought from CMIP5 models. Sci. Rep. 9 (1), 1–12. https://doi.org/10.1038/s41598-019-41196-z.

Mahmood, R., Pielke Sr, R.A., Hubbard, K.G., Niyogi, D., Dirmeyer, P.A., McAlpine, C., Fall, S., 2014. Land cover changes and their biogeophysical effects on climate. Int. J. Climatol. 34 (4), 929–953. https://doi.org/10.1002/joc.3736.

McKee, T. B., Doesken, N. J., and Kleist, J. (1993). The relationship of drought frequency and duration to time scales. In Proceedings of the 8th Conference on Applied Climatology. Vol. 17, No. 22, pp. 179-183.

Miralles, D.G., Teuling, A.J., Van Heerwaarden, C.C., Vilà-Guerau de Arellano, J., 2014. Mega-heatwave temperatures due to combined soil desiccation and atmospheric heat accumulation. Nat. Geosci. 7 (5), 345–349. https://doi.org/10.1038/NGEO2141.

Mishra, A.K., Singh, V.P., 2010. A review of drought concepts. J. Hydrol. 391 (1–2), 202–216. https://doi.org/10.1016/j.jhydrol.2010.07.012.

Mo, K.C., 2011. Drought onset and recovery over the United States. J. Geophys. Res. Atmos. 116 (D20) https://doi.org/10.1029/2011. JD016168.

Mondal, S., Mishra, K.A., Leung, R., Cook, B., 2023. Global droughts connected by linkages between drought hubs. Nat. Commun. 14 (1), 144. https://doi.org/10.1038/s41467 -022-35531-8.

Muñoz-Sabater, J., Dutra, E., Agustí-Panareda, A., Albergel, C., Arduini, G., Balsamo, G., et al., 2021. ERA5-Land: A state-of-the-art global reanalysis dataset for land applications. Earth Syst. Sci. Data 13 (9), 4349–4383. https://doi.org/10.5194/essd-13-4349-2021.

Pelosi, A., Terribile, F., D'Urso, D., Chirico, G., 2020. Comparison of ERA5-land and UERRA MESCAN-SURFEX reanalysis data with spatially interpolated weather observations for the regional assessment of reference evapotranspiration. Water 12 (6), 1669. https://doi.org/10.3390/w12061669.

Pinzon, J.E., Tucker, C.J., 2014. A non-stationary 1981–2012 AVHRR NDVI3g time series. Remote Sens. (Basel) 6 (8), 6929–6960. https://doi.org/10.3390/rs6086929.

Pongratz, J., Reick, C., Raddatz, T., Claussen, M., 2008. A reconstruction of global agricultural areas and land cover for the last millennium. Global Biogeochem. Cycles 22 (3), GB3018. https://doi.org/10.1029/2007GB003153.

Poulter, B., Frank, D., Ciais, P., Myneni, R.B., Andela, N., Bi, J., van der Werf, G.R., 2014. Contribution of semi-arid ecosystems to interannual variability of the global carbon cycle. Nature 509 (7502), 600–603.

Ramankutty, N., Foley, J.A., 1999. Estimating historical changes in global land cover: croplands from 1700 to 1992. Global Biogeochem. Cycles 13 (4), 997–1027. https://doi.org/10.1029/1999GB900046.

Reichstein, M., et al., 2013. Climate extremes and the carbon cycle. Nature 500, 287–295.

Rousi, E., Kornhuber, K., Beobide-Arsuaga, G., Luo, F., Coumou, D., 2022. Accelerated western european heatwave trends linked to more-persistent double jets over Eurasia. Nat. Commun. 13 (1), 3851. https://doi.org/10.1038/s41467-022-31432-y.

Scherrer, D., Bader, M.K.F., Körner, C., 2011. Drought-sensitivity ranking of deciduous tree species based on thermal imaging of forest canopies. Agric. For. Meteorol. 151 (12), 1632–1640.

Seneviratne, S.I., Corti, T., Davin, E.L., Hirschi, M., Jaeger, E.B., Lehner, I., et al., 2010. Investigating soil moisture–climate interactions in a changing climate: a review. Earth Sci. Rev. 99 (3–4), 125–161. https://doi.org/10.1016/j.earscirev.2010.02.004.

Sheffield, J., Goteti, G., Wen, F., Wood, E.F., 2004. A simulated soil moisture based drought analysis for the United States. J. Geophys. Res. Atmos. 109 (D24).

Smith, C., Baker, J.C.A., Spracklen, D.V., 2023. Tropical deforestation causes large reductions in observed precipitation. Nature 615 (7951), 270–275. https://doi.org/10.1038/s41586-022-05690-1.

Sun, H., Xu, Z., Liu, H., 2023. An evaluation of the response of vegetation greenness, moisture, fluorescence, and temperature-based remote sensing indicators to drought stress. J. Hydrol. 625, 130125.

Tucker, C.J., Pinzon, J.E., Brown, M.E., Slayback, D.A., Pak, E.W., Mahoney, R., El Saleous, N., 2005. An extended AVHRR 8-km NDVI dataset compatible with MODIS and SPOT vegetation NDVI data. Int. J. Remote Sens. 26 (20), 4485–4498. https://doi.org/10.1080/01431160500168 686.

Van Loon, A.F., Van Lanen, H.A., 2013. Making the distinction between water scarcity and drought using an observation-modeling framework. Water Resour. Res. 49 (3), 1483–1502. https://doi.org/10.1002/wrcr.20147.

Vogel, M.M., Orth, R., Cheruy, F., Hagemann, S., Lorenz, R., van den Hurk, B.J., Seneviratne, S.I., 2017. Regional amplification of projected changes in extreme temperatures strongly controlled by soil moisture-temperature feedbacks. Geophys. Res. Lett. 44 (3), 1511–1519. https://doi.org/10.1002/2016 GL071235.

Wang, W. Y. (2014). The study on evaporation and effective precipitation in semi-arid region. Lanzhou University. (In Chinese) Retrieved from https://kns.cnki.net/%20KCMS/detail/detail.aspx?dbname=CMFD201402%26filename=1014301865.nh.

Weber, K., Stewart, M., 2004. A critical analysis of the cumulative rainfall departure concept. Ground Water 42 (6/7), 935.

Wei, J., Dinneyer, P.A., Guo, Z., 2008. Sensitivities of soil wetness simulation to uncertainties in precipitation and radiation. Geophys. Res. Lett. 35 (15), LI5703. https://doi.org/10.1029/2008GL034494.

Xu, Y., Zhang, X., Hao, Z., Singh, V.P., Hao, F., 2021. Characterization of agricultural drought propagation over China based on bivariate probabilistic quantification. J. Hydrol. 598, 126194 https://doi.org/10.1016/j.jhydrol.2021.126194.

Yan, H., Wang, S.Q., Wang, J.B., Lu, H.Q., Guo, A.H., Zhu, Z.C., Shugart, H.H., 2016. Assessing spatiotemporal variation of drought in China and its impact on agriculture during 1982–2011 by using PDSI indices and agriculture drought survey data. J. Geophys. Res. Atmos. 121 (5), 2283–2298.

Yang, X., Zhang, M., He, X., Ren, L., Pan, M., Yu, X., Sheffield, J., 2020. Contrasting influences of human activities on hydrological drought regimes over China based on high-resolution simulations. Water Resour. Res. 56 (6), e2019WR025843.

Yang, X., Ma, H., Wu, F., Zhang, M., Zhang, L., Yuan, S., 2023. (2023) spatiotemporal evolution of global and arid zone drought based on CMIP6. Water Resources Protection. 02, 40–49. In Chinese.

Yin, J., Gentine, P., Slater, L., Gu, L., Pokhrel, Y., Hanasaki, N., Schlenker, W., 2023. Future socio-ecosystem productivity threatened by compound drought–heatwave events. Nat. Sustainability 1–14. https://doi.org/10.1038/s41893-022-01024-1.

Zhang, L., Dawes, W., Walker, G., 2001. Response of mean annual evapotranspiration to vegetation changes at catchment scale. Water Resour. Res. 37 (3), 701–708. https://doi.org/10.1029/2000WR900325.

Zhang, H., Ding, J., Wang, Y., Zhou, D., Zhu, Q., 2021a. Investigation about the correlation and propagation among meteorological, agricultural and groundwater droughts over humid and arid/semi-arid basins in China. J. Hydrol. 603, 127007 https://doi.org/10.1016/j.jhydrol.2021.127007.

Zhang, Y., Hao, Z., Feng, S., Zhang, X., Xu, Y., Hao, F., 2021b. Agricultural drought prediction in China based on drought propagation and large-scale drivers. Agric Water Manag 255, 107028. https://doi.org/10.1016/j.agwat. 2021.107028.

Zhang, X., Hao, Z., Singh, V.P., Zhang, Y., Feng, S., Xu, Y., Hao, F., 2022c. Drought propagation under global warming: characteristics, approaches, processes, and controlling factors. Sci. Total Environ. 838, 156021 https://doi.org/10.1016/j.scitotenv.2022.156021.

Zhang, H., Henderson-Sellers, A., McGuffie, K., 1996. Impacts of tropical deforestation. part I: process analysis of local climatic change. J. Clim. 9 (7), 1497–1517. https://doi.org/10.1175/1520-0442(1996)009<1497. IOTDPI> 2.0.CO;2.

Zhang, Q., Miao, C., Gou, J., Wu, J., Jiao, W., Song, Y., Xu, D., 2022b. Spatiotemporal characteristics of meteorological to hydrological drought propagation under natural conditions in China. Weather Clim. Extremes 38, 100505. https://doi.org/10.1016/j.wace.2022.100505.

Zhang, Y., Song, X., 2015. Techniques of abrupt change detection and trends analysis in hydroclimatic time-series: advances and evaluation. Arid Land Geography 38 (4), 652–665.

Zhang, M., Yang, X., Pan, M., Zhang, L., Fang, X., Sheffield, J., 2023. Spatio-temporal characteristics and driving factors of the meteorological drought across China based on CMIP6. Hydrol. Res. 54 (3), 382–400.

Zhang, Y., Ye, A., Nguyen, P., Analui, B., Sorooshian, S., Hsu, K., 2022a. QRF4P-NRT: Probabilistic Post-processing of Near-real-time Satellite Precipitation Estimates using Quantile Regression Forests. Water Resour. Res. 032 117. https://doi.org/10.1029/2022WR e2022WR032117.

Zhang, X., Yu, P., Wang, D., Xu, Z., 2022d. Density-and age-dependent influences of droughts and intrinsic water use efficiency on growth in temperate plantations. Agric. For. Meteorol. 325, 109134.

Zhao, J., Zhang, Q., Zhu, X., Shen, Z., Yu, H., 2020. Drought risk assessment in China: evaluation framework and influencing factors. Geogr. Sustain. 1, 220–228.

Zhou, J., Li, Q., Wang, L., Lei, L., Huang, M., Xiang, J., Zhu, G., 2019. Impact of climate change and land-use on the propagation from meteorological drought to hydrological drought in the eastern Qilian Mountains. Water 11 (8), 1602. https://doi.org/10.3390/w11081602.

Zhou, K., Li, J., Zhang, T., Kang, A., 2021a. The use of combined soil moisture data to characterize agricultural drought conditions and the relationship among different drought types in China. Agric Water Manag 243, 106479. https://doi.org/10.1016/j.agwat.2020.106479.

Zhou, Z., Shi, H., Fu, Q., Ding, Y., Li, T., Liu, S., 2021b. Investigating the propagation from meteorological to hydrological drought by introducing the nonlinear dependence with directed information transfer index. Water Resour. Res. 57 (8), e2021WR030028 https://doi.org/10.1029/2021WR030028.

Zhou, S., Yu, B., Zhang, Y., 2023. Global concurrent climate extremes exacerbated by anthropogenic climate change. Sci. Adv. 9 (10), eabo1638 https://doi.org/10.1126/sciadv.abo1638.

Zhu, Y., Liu, Y., Wang, W., Singh, V.P., Ren, L., 2021. A global perspective on the probability of propagation of drought: from meteorological to soil moisture. J. Hydrol. 603, 126907 https://doi.org/10.1016/j.jhydrol.2021.126 907.